Features of Chaotic Transients in Excitable Media Governed by Spiral and Scroll Waves

Thomas Lilienkamp,[1,2,*] Jan Christoph,[1] and Ulrich Parlitz[1,2]
[1]Max Planck Institute for Dynamics and Self-Organization, Am Fassberg 17, 37077 Göttingen, Germany
[2]Institute for Nonlinear Dynamics, Georg-August-Universität Göttingen, Friedrich-Hund-Platz 1, 37077 Göttingen, Germany
(Received 19 February 2017; revised manuscript received 16 May 2017; published 31 July 2017)

In excitable media, chaotic dynamics governed by spiral or scroll waves is often not persistent but transient. Using extensive simulations employing different mathematical models we identify a specific type-II supertransient by an exponential increase of transient lifetimes with the system size in 2D and an investigation of the dynamics (number and lifetime of spiral waves, Kaplan-Yorke dimension). In 3D, simulations exhibit an increase of transient lifetimes and filament lengths only above a critical thickness. Finally, potential implications for understanding cardiac arrhythmias are discussed.

DOI: 10.1103/PhysRevLett.119.054101

Chaotic behavior of dynamical systems is a widespread and well-studied phenomenon. It can be observed in a large diversity of systems from simple low-dimensional regimes up to complex and high-dimensional dynamics. However, in many cases it is of great interest whether the observed chaotic dynamics (both in theoretical models and experiments) are persistent or temporary. From a nonlinear dynamics point of view, the dynamics of the latter one is usually determined by chaotic saddles or repellers, whereas persistent chaos is governed by a chaotic attractor. In practice, chaotic transients occur in various fields like ecology [1], particle advection [2], or chemical reactions [3]. In fact, the difference between transient and persistent chaos can be vital in medicine: In cardiology, cardiac arrhythmias (like ventricular fibrillation) can be associated with highly chaotic spatiotemporal wave dynamics inside the heart [4–7], which is lethal in many cases due to the dysfunctional pumping function. Distinguishing between persistent and transient arrhythmias is thus essential, and it may, in the future, have an impact on the medical treatment and risk assessment of cardiac arrhythmias.

In this work we investigate chaotic transients in extended reaction-diffusion systems of excitable media using two different numerical models that describe the action potential propagation in cardiac tissue: The Aliev-Panfilov model [8] is a two-variable model (five parameters) for cardiac excitation, described by the equations

$$\frac{\partial u}{\partial t} = \nabla \cdot \underline{D} \nabla u - ku(1-u)(a-u) - uv, \tag{1}$$

$$\frac{\partial v}{\partial t} = \epsilon(u,v)[-v - ku(u-a-1)], \tag{2}$$

$$\epsilon(u,v) = \epsilon_0 + \frac{\mu_1 v}{u+\mu_2}. \tag{3}$$

The Fenton-Karma model [9] [Eqs. (4)–(5)] is a three variable model with fourteen parameters, which comprises an approach for modeling the ion channel dynamics of a cell:

$$\frac{\partial u}{\partial t} = \nabla \underline{D} \nabla u - I_{\mathrm{ion}}(u, \mathbf{h})/C_m, \tag{4}$$

$$\frac{\partial \mathbf{h}}{\partial t} = \mathbf{g}(u, \mathbf{h}). \tag{5}$$

The detailed equations that describe the ionic currents I_{ion} in Eq. (4), and the evolution equations for the gating variables $\mathbf{h} = (v, w)$ [Eq. (5)], can be found in the Supplemental Material [10].

In both models, the first term in Eqs. (1) and (4), respectively, describes the diffusive part of the dynamic system. In our simulations, a scalar and homogeneous diffusion tensor was chosen ($\underline{D} = D = 0.2$). The differential equations, Eqs. (1)–(3) and Eqs. (4)–(5), were solved on a spatial grid (with a model specific spacing constant h) using an explicit Euler scheme with no-flux boundary conditions.

Different choices of parameters cause diverse behavior of spiral or scroll waves (concerning, for example, breakup mechanisms or spiral tip trajectories) [11]. In order to investigate whether properties related to the transient nature of the chaotic dynamics are robust under a change of the local cell dynamic model, and also under a change of parameters, we investigate three distinct cell dynamics: the Aliev-Panfilov model [Eqs. (1)–(3)] from now on abbreviated with **AP** (solved using a spacing constant $h = 0.8$ and $dt = 0.2$), and the Fenton-Karma model [Eqs. (4)–(5)], using two different parameter sets (all simulation parameters can be found in the Supplemental Material [10]), from now on abbreviated with **FK1** (with $h = 1.0$ and $dt = 0.2$) and **FK2** (with $h = 1.5$ and $dt = 0.1$), respectively. Both sets of parameters (**FK1** and **FK2**) were investigated in [11] and create a spiral wave breakup by different mechanisms [biphasic action potential duration (APD) restitution curve, and supernormal conduction

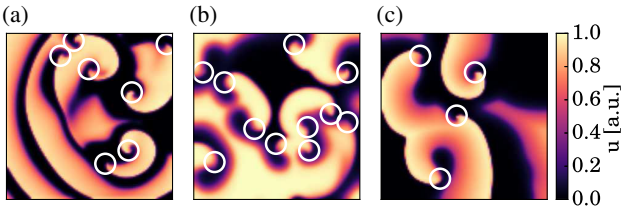

FIG. 1. Snapshots of the spatiotemporal dynamics for the three investigated systems **AP** (a), **FK1** (b), and **FK2** (c) (domain sizes $L_x \times L_y$ of 80×80, 100×100 and 150×150, respectively). (White) circles indicate the phase singularities (organizing centers) of the spiral waves.

velocity, respectively]. Figure 1 shows snapshots of the chaotic dynamics (variable u) of the discussed models (**AP**, **FK1**, and **FK2**) in a rectangular two-dimensional domain.

The escape rate κ is the quantity that measures how fast random initial conditions (which are governed by the chaotic dynamics) escape the chaotic saddle and reach the final (nonchaotic) state. By generating many initial conditions and determining the fraction that still shows chaotic dynamics at time t, $N_{\mathrm{Ch}}(t)$, the escape rate κ can be extracted, since this quantity typically decreases exponentially in time with $N_{\mathrm{Ch}}(t) \sim \exp(-\kappa t)$ [12].

As a first step, we investigated the role of the system size in 2D simulations. In [13] two types of supertransients (systems where the escape rate decreases rapidly with the system size) are distinguished. In systems of type-I supertransients (nonstationary transients), the number of objects which are essential for the chaotic dynamics (e.g., "defects" or "regions of turbulence") decreases in time, and the dynamics converge over time to the final state. For this class of systems, the dependence of the escape rate κ on the system size L can usually be described by a power law [Eq. (6), with $\beta > 0$]. In systems that show transients of type-II in comparison, the transition to the final attractor is abrupt, and cannot usually be predicted by quantities like time series. The escape rate κ increases exponentially with the system size L [Eq. (7), with the parameters $a > 0$ and $\gamma > 0$],

$$\kappa(L) \sim L^{-\beta}, \tag{6}$$

$$\kappa(L) \sim \exp(-aL^{\gamma}). \tag{7}$$

Instead of the escape rate κ in the following the inverse escape rate is considered, which is an estimate for the average transient lifetime $\langle T \rangle \approx 1/\kappa$ [12].

In 2D simulations on a rectangular domain, the average transient lifetime was determined for various sizes of the 2D simulation area. While keeping the grid spacing h constant for each model, the simulation domain $L_x \times L_y = (N_x h) \times (N_y h)$ was increased by changing the number of grid points ($N_x \times N_y \in [80\times80, 90\times90, 100\times100, 110\times110, 120\times120, 130\times130]$). For each domain size, 3000 initial conditions were

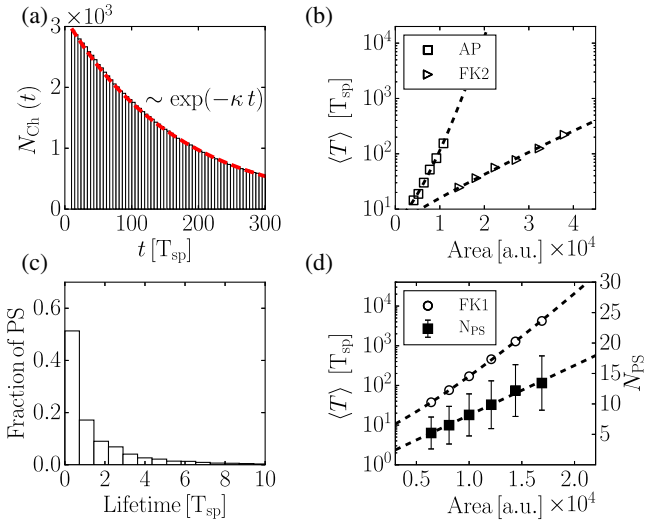

FIG. 2. Chaotic transients and the average lifetime in 2D simulations. In subplot (a) $N_{\mathrm{Ch}}(t)$ is shown over time [measured in spiral rotations (T_{sp})] for an exemplary domain size of $L_x \times L_y = 100 \times 100$ using the **FK1** model. The average transient lifetime $\langle T \rangle \approx 1/\kappa$ can be extracted by fitting the exponential decay [(red) dashed line]. In (b) the average transient lifetimes are plotted for various system sizes for both models: **AP** (open square) and **FK2** (right pointed triangle). For **FK1**, the lifetime distribution of phase singularities for a simulation domain of $L_x \times L_y = 100 \times 100$ was determined (c) as well as the mean number of phase singularities N_{PS} (filled square) and the average transient lifetime $\langle T \rangle$ (open circle) for various area sizes (d).

created (details about the induction protocol can be found in the Supplemental Material [10]). Self-termination of a simulation was declared when the overall excitation (dynamic variable u) came below a threshold ($(1/L_x \times L_y)\sum_{i,j} u_{ij} < 0.001$). For the determination of $\langle T \rangle$ from $N_{\mathrm{Ch}}(t)$ an initial amount of time, which is equal to 10 spiral periods, was discarded. The average transient lifetime was determined for all three models (**AP**, **FK1**, **FK2**) for the different domain sizes.

Figure 2(a) shows $N_{\mathrm{Ch}}(t)$ exemplary for **FK1** and a domain size of $L_x \times L_y = 100 \times 100$. An exponential scaling of the average transient lifetime with the domain size (area $= L_x \times L_y$) in 2D was confirmed in all three models [Fig. 2(b) for **FK2** and **AP**, and Fig. 2(d) for **FK1**, respectively]. In fact, supertransients of type-II were identified with coefficients $\gamma_{\mathrm{AP}} = 1.3843 \pm 4.2 \times 10^{-3}$, $\gamma_{\mathrm{FK1}} = 1.2274 \pm 6.9 \times 10^{-4}$, $\gamma_{\mathrm{FK2}} = 0.8813 \pm 2.8 \times 10^{-2}$, $a_{\mathrm{AP}} = 4.5851 \times 10^{-6} \pm 8.6 \times 10^{-11}$, $a_{\mathrm{FK1}} = 4.4123 \times 10^{-5} \pm 1.3 \times 10^{-10}$ and $a_{\mathrm{FK2}} = 7.1151 \times 10^{-4} \pm 1.5 \times 10^{-6}$. It is noteworthy, that the actual scaling parameter γ is not only determined by the choice of the cell model (Aliev-Panfilov, Fenton-Karma) but also sensitively depends on the choice of model parameters.

The identification of supertransients of type-II can also be confirmed in the underlying dynamics of the investigated excitable systems: The chaotic dynamics are

mainly determined by spiral waves in two-dimensional (2D) systems or scroll waves in three-dimensional (3D) systems. The number of the organizing centers of these waves fluctuates during a chaotic episode due to pairwise creation or annihilation of phase singularities (tips of the spirals), wave breakup, or collisions with the boundary. The dynamics terminate (without any impact from outside), if at some point in time every spiral wave annihilates with another spiral wave or the boundary. Only plane waves remain without any phase singularity and the excitation dies out; thus, the chaotic episode has finished and the system remains in the (stable) attractor given by a nonexcited medium (see the Supplemental Material for the course of such a self termination [14]). During such an episode, the number of spiral waves, or their corresponding phase singularities (which play the role of the "defect" here), does not decrease over time, but fluctuates due to the creation and annihilation mechanisms. The lifetime distribution of a single phase singularity for **FK1** and a simulation domain of $L_x \times L_y = 100 \times 100$ is shown in Fig. 2(c), indicating that the dynamics are not dominated by single long-living spiral waves but characterized by a constant production and annihilation of relatively short-living phase singularities. As already noted by Strain and Greenside [15], the final collapse of the system occurs then, abruptly, and no obvious indications for the upcoming termination can be found. For exemplary time series of the number of phase singularities N_{PS} and the pseudo ECG before the collapse of the dynamics, as well as details of the detection of the phase singularities, see [10].

When the simulation area is extended, the mean number of phase singularities (and thus the number of spiral waves) increases linearly [Fig. 2(d)], which is in accordance with the findings that spiral waves occupy finite amounts of the area, also called "tiles" [5,16]. The lifetime distribution of single spirals does not change with the system size (mean lifetime of spiral waves $\langle T_{\mathrm{PS}} \rangle = 4.49, 4.37, 4.48, 4.45, 4.54, 4.53\ \mathrm{T_{sp}}$ for $L_x = 80$, 90, 100, 110, 120, 130). Using a Markovian approach for the dynamics (each state characterized by the number of phase singularities), and assuming that the transition probability to a state with no spiral waves is decreasing exponentially with the number of spiral waves (which grows linearly with the system size), one can reasonably deduce the exponential scaling of the transient lifetime with the system size here [17]. From this point of view, the scaling parameters a and γ can be related to the lifetime of the spiral waves and the number or the size of single spiral waves compared to the domain size.

Apart from the average transient lifetime, which is a characteristic feature of the transient nature, we focus in the following on the chaotic properties of the dynamics. In systems which exhibit chaotic transients, an initial condition after a finite amount of time will end up in another attractor (which actually can also be chaotic). However,

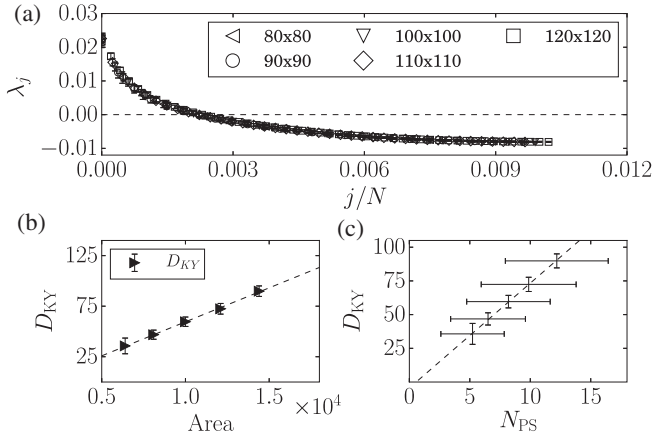

FIG. 3. The chaotic features of the dynamics using **FK1**. Analysis of the Lyapunov density for various system sizes (a), Kaplan-Yorke dimension D_{KY} (filled triangles) versus the system size (b) and D_{KY} versus N_{PS} (c).

dynamic invariants that are used for "classical" (persistent) chaotic systems can, in some cases, also be used for characterizing the transients. For example, Lyapunov exponents can, in practice, also be calculated in systems with finite chaotic episodes. Because Lyapunov exponents are mathematically defined on an infinite time scale, we refer to "finite time Lyapunov exponents" when we speak of Lyapunov exponents of chaotic transients [12]. Technically, there is no difference in the calculation scheme, except that the calculation stops before the self termination of the dynamics. However, in practice this is only meaningful if the transients provide enough time for the convergence of the estimates of the exponents.

The Lyapunov spectrum provides information about how chaotic the dynamics are before self termination. We investigated how these properties of the dynamics change with an increasing system size (details can be found in the Supplemental Material [10]). Figure 3(a) depicts the Lyapunov density ([12,18]) (jth Lyapunov exponent versus j divided by system size $N = N_x \times N_y$). The Lyapunov exponents for different system sizes clearly align with each other, which implies that the number of positive or negative Lyapunov exponents scales with the system size (extensive chaos).

Furthermore, in order to assess the chaotic dynamics, the Kaplan-Yorke dimension D_{KY} was calculated for various system sizes based on the Lyapunov spectrum [19]. Figure 3(b) shows that the Kaplan-Yorke dimension D_{KY} grows linearly with the system size (triangles). Since the number of phase singularities (equivalent to the number of spiral waves) also grows linearly [Fig. 2(d)], we can identify a mean D_{KY} per spiral wave of $\approx 7.77 \pm 0.12$. Although studies indicate that parts of the degrees of dynamic freedom in spatiotemporal chaos in excitable media are not related to the defects (spiral cores) [20], we can conclude that the degree of chaos

(Kaplan-Yorke dimension) can be estimated by the number of spiral waves permitted by the respective system size [see Fig. 3(c)].

Similarly to [21], we also found that noise has an impact on the average lifetime. Details regarding the results can be found in the Supplemental Material [10].

As a next step, the average transient lifetime was also determined in 3D domains. In three dimensions, spiral waves correspond to scroll waves, whereas the former pointlike phase singularities that mark the tip of a spiral wave correspond to filamentlike one-dimensional curves in 3D. Scroll waves can be considered as "stacked spiral waves," where the curvature and the meandering behavior of the filament are essential for the dynamics. In particular, we are interested in how the average transient lifetime changes when extending the 2D dimensional domain step by step to 3D. For this purpose, the initial 2D simulations with $L_x \times L_y = (80h) \times (80h)$ were gradually extended in the third dimension L_z (from now on denoted as "thickness"). As in [22], in all three models, a critical thickness in the third dimension could be established up to which the average transient lifetime remains approximately constant (see Fig. 4). Above this threshold, the average transient lifetime increases exponentially.

In order to find the dynamic origin for this critical thickness, the filaments (the organizing centers) of the scroll waves were also detected. Details about the detection of the filaments can be found in the Supplemental Material [10]. In Figs. 4(a), 4(c), and 4(e) the average transient lifetime $\langle T \rangle$ is compared to the average number of filaments, N_{fila}, for each thickness of the domain. In all three models, the critical thickness in the average transient lifetime is also pronounced in terms of the number of filaments N_{Fila}. In addition, the average length of the filaments per thickness (ALF/L_z) was also determined. In the case of straight filaments only aligned along the third dimension of the system, this quantity is equal to one. Thus, deviations from a constant value provide information about deviating filament alignment. In "thin" systems, the domain only provides enough space for filaments aligning along the third dimension (thus, the system is quasi-2D). The approximately constant ratio ALF/L_z for lower thicknesses indicates that most filaments are aligned along the third dimension [crosses in Fig. 4(b) (**AP**), 4(d) (**FK1**), and 4(f) (**FK2**)]. In larger domains, for **AP** and **FK1**, the critical thickness can also be recognized by ALF/L_z (smeared out for **FK2**). However, for bigger systems, ALF/L_z saturates in all three models (or even slightly decreases for **AP** and **FK1**), indicating that the maximum (average) filament length is (model dependent) confined. The presence of the critical thickness in both quantities (N_{fila} and ALF/L_z) suggests that above the critical thickness, filaments break up (due to a negative filament tension in all models [9,23]). This transition from vertically arranged filaments to actual scroll wave turbulence above a critical thickness of the substrate

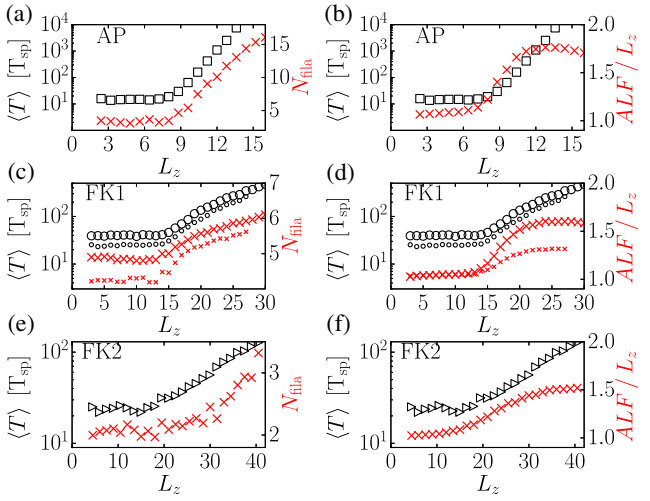

FIG. 4. Chaotic transients in 3D domains. A critical thickness in the third dimension of the simulation grids exists in all three models, below which the average transient lifetime remains approximately constant [**AP**: (square) in (a) and (b), **FK1**: (circle) (small circles for simulations using the doubled resolutions) in (c) and (d) and **FK2**: (right-pointing triangle) in (e) and (f)]. The dynamic origin of the critical thickness concerning the average transient lifetime can be identified with the average number of filaments (N_{fila}) in the system, which is rapidly increasing above the critical thickness [(crosses) in (a) (**AP**), (c) (**FK1**, small crosses for simulations using doubled resolutions) and (e) (**FK2**)]. The average length of the filaments divided by the thickness (ALF/L_z) also exhibits the critical thickness, but saturates for larger domains [(crosses) in (b) (**AP**), (d) (**FK1**, small crosses for simulations using the doubled resolutions) and (f) (**FK2**)].

was also observed by Dierckx *et al.* [24]. However, the saturation of ALF/L_z leads to the conclusion that the increase of the average transient lifetime is mainly based on the pure number of filaments (equivalent to the number of spiral waves in 2D) and does not depend significantly on the length of the filaments. In order to investigate finite size effects, all simulations were repeated in the case of **FK1** with a doubled resolution [$h \to h/2$, small circles and crosses in Figs. 4(c) and 4(d)]. Quantitative differences in the absolute numbers (e.g., N_{fila}) are visible, but the main qualitative findings (in particular the critical thickness) are robust under a doubling of the spatial resolution.

We have shown that chaotic transients are a robust phenomenon in excitable media and occur similarly in different numerical models (Aliev-Panfilov model and Fenton-Karma model) of excitable systems with different underlying mechanisms for spiral wave breakup. The average lifetimes of chaotic transients depend on the system size, in both two and three dimensions, and are influenced by the addition of low amplitude noise. We found in the investigated excitable systems, that spiral or scroll waves, and their corresponding phase singularities or filaments, are the main topological objects that promote the duration of chaotic episodes.

Our findings agree with the general notion that larger heart muscle volumes increase the risk of cardiac arrhythmias and related morbidity and mortality [25–27]. Our results suggest that larger volumes can possibly contain a larger number of phase singularities, and therefore, not only increase the transient lifetimes, but also enhances the spatiotemporal complexity of the chaotic dynamics, which may have an impact on the success rates of defibrillation attempts [28,29]. In particular, the role of the critical thickness investigated in the 3D simulations may be of further interest in this context. Cardiac hypertrophy, for instance, is accompanied by an increase in heart muscle volume. Even though the overall number of cardiac cells does not change in hypertrophic hearts, other factors, such as altered excitation thresholds and conduction velocities, may lead to an effective scaling of the size of the excitable system with respect to the sizes of dynamic structures like spiral or scroll waves present in the system. In fact, from this point of view, the administration of certain antiarrhythmic agents could be interpreted as a change of properties of the cardiac tissue in order to promote early self-termination of cardiac arrhythmias [30]. With respect to transient lifetimes, phenomenological modeling could provide a generalized framework for investigating the influence of cardiac substrate changes onto the persistence of cardiac arrhythmias.

We thank the International Max Planck Research School (IMPRS) for Physics of Biological and Complex Systems (PBCS), the Federal Ministry of Education and Research (BMBF, FKZ031A147, GO-Bio), the German Centre for Cardiovascular Research (DZHK e.V.), the "Deutsche Forschungsgemeinschaft (DFG, Collaborative Research Centers SFB1002 "Modulatory Units in Heart Failure", project C03 and SFB937 "Collective Behavior of Soft and Biological Matter", project A18) for financial support. Furthermore, we thank Stefan Luther and Sebastian Berg for fruitful discussions and continuous support.

*thomas.lilienkamp@ds.mpg.de

[1] K. McCann and P. Yodzis, Am. Nat. **144**, 873 (1994).
[2] J. J. B. Biemond, A. P. S. de Moura, G. Károlyi, C. Grebogi, and H. Nijmeijer, Phys. Rev. E **78**, 016317 (2008).
[3] A. M. Barr, K. Na, L. E. Reichl, and C. Jung, Phys. Rev. E **79**, 026215 (2009).
[4] J. M. Davidenko, A. V. Pertsov, R. Salomonsz, W. Baxter, and J. Jalife, Nature (London) **355**, 349 (1992).
[5] R. A. Gray, A. M. Pertsov, and J. Jalife, Nature (London) **392**, 75 (1998).
[6] F. X. Witkowski, L. J. Leon, P. A. Penkoske, W. R. Giles, M. L. Spano, W. L. Ditto, and A. T. Winfree, Nature (London) **392**, 78 (1998).
[7] E. M. Cherry and F. H. Fenton, New J. Phys. **10**, 125016 (2008).
[8] R. R. Aliev and A. V. Panfilov, Chaos Solitons Fractals **7**, 293 (1996).
[9] F. Fenton and A. Karma, Chaos **8**, 20 (1998).
[10] See Supplemental Material at http://link.aps.org/supplemental/10.1103/PhysRevLett.119.054101 for evolution equations of the Fenton-Karma model, simulation parameters, technical details of the simulations, and further results.
[11] F. H. Fenton, E. M. Cherry, H. M. Hastings, and S. J. Evans, Chaos **12**, 852 (2002).
[12] Y.-C. Lai and T. Tél, *Transient Chaos*, Applied Mathematical Sciences (Springer New York, New York, NY, 2011), Vol. 173.
[13] J. P. Crutchfield and K. Kaneko, Phys. Rev. Lett. **60**, 2715 (1988).
[14] See Supplemental Material at http://link.aps.org/supplemental/10.1103/PhysRevLett.119.054101 for the course of such a self termination on a 100×100 grid using the FK1 model.
[15] M. C. Strain and H. S. Greenside, Phys. Rev. Lett. **80**, 2306 (1998).
[16] G. Byrne, C. D. Marcotte, and R. O. Grigoriev, Chaos **25**, 033108 (2015).
[17] K. Sugimura and H. Kori, Phys. Rev. E **92**, 062915 (2015).
[18] *Dynamical Systems Approach to Turbulence*, edited by T. Bohr, Cambridge Nonlinear Science Series Vol. 8 (Cambridge University Press, Cambridge, New York, 1998).
[19] J. L. Kaplan and J. A. Yorke, in *Functional Differential Equations and Approximation of Fixed Points*, edited by H.-O. Peitgen and H.-O. Walther (Springer, Berlin, Heidelberg, 1979), Vol. 730, pp. 204–227.
[20] D. A. Egolf, Phys. Rev. Lett. **81**, 4120 (1998).
[21] R. Wackerbauer and S. Kobayashi, Phys. Rev. E **75**, 066209 (2007).
[22] Z. Qu, Am. J. Physiol. **290**, H255 (2005).
[23] V. N. Biktashev, A. V. Holden, and H. Zhang, Phil. Trans. R. Soc. A **347**, 611 (1994).
[24] H. Dierckx, H. Verschelde, Ö. Selsil, and V. N. Biktashev, Phys. Rev. Lett. **109**, 174102 (2012).
[25] J. M. McLenachan, E. Henderson, K. I. Morris, and H. J. Dargie, N. Engl. J. Med. **317**, 787 (1987).
[26] T. Kahan, Heart and lung **91**, 250 (2005).
[27] A. Verma, A. Meris, H. Skali, J. K. Ghali, J. M. O. Arnold, M. Bourgoun, E. J. Velazquez, J. J. McMurray, L. Kober, M. A. Pfeffer, R. M. Califf, and S. D. Solomon, JACC Cardiovasc. Imaging **1**, 582 (2008).
[28] N. Bajaj, L. Leon, S. Kimber, and E. Vigmond, *Proceedings of the Annual Conference on Engineering in Medicine and Biology, Shanghai, China, 2005* (IEEE, Shanghai, 2005), pp. 7208–7211.
[29] G. Plank, L. J. Leon, S. Kimber, and E. J. Vigmond, J. Cardiovasc. Electrophysiol. **16**, 205 (2005).
[30] M. Yamazaki, H. Honjo, H. Nakagawa, Y. S. Ishiguro, Y. Okuno, M. Amino, I. Sakuma, K. Kamiya, and I. Kodama, Am. J. Physiol. **292**, H539 (2006).